In-tunnel vehicular radio channel characterization

Bernadó, Laura; Roma, Anna; Paier, Alexander; Zemen, Thomas; Czink, Nicolai; Kåredal, Johan; Thiel, Andreas; Tufvesson, Fredrik; Molisch, Andreas; Mecklenbrauker, Christoph

Published in:
[Host publication title missing]

DOI:
10.1109/VETECS.2011.5956510

2011

In-Tunnel Vehicular Radio Channel Characterization

Laura Bernadó[1], Anna Roma[1], Alexander Paier[2], Thomas Zemen[1], Nicolai Czink[1], Johan Karedal[3], Andreas Thiel[4], Fredrik Tufvesson[2], Andreas F. Molisch[5], Christoph F. Mecklenbräuker[3]

[1]Forschungszentrum Telekommunikation Wien (FTW), Vienna, Austria
[2]Institute of Telecommunications, Vienna University of Technology, Vienna, Austria
[3]Department of Electrical and Information Technology, Lund University, Lund, Sweden
[4]Delphi Delco Electronics Europe GmbH, Bad Salzdetfurth, Germany
[5]Department of Electrical Engineering, University of Southern California, Los Angeles, CA, USA
Contact: bernado@ftw.at

***Abstract*—Inside a tunnel, electromagnetic wave propagation differs strongly from the well understood "open-air" situation. The characterization of the tunnel environment is crucial for deploying vehicular communication systems. In this paper we evaluate vehicle-to-vehicle (V2V) radio channel measurements inside a tunnel. We estimate the time-varying root mean square (rms) delay and Doppler spreads, as well as the excess delay and the maximum Doppler dispersion. The fading process in V2V communications is inherently non-stationary. Hence, we characterize the stationarity time, for which we can consider the fading process to be wide sense stationary.**

We show that the spreads, excess delay, and maximum Doppler dispersion are larger on average when both vehicles are inside the tunnel compared to the "open-air" situation. The temporal evolution of the stationarity time is highly influenced by the strength of time-varying multipath components and the distance between vehicles. Furthermore, we show the good fit of the rms delay and Doppler spreads to a lognormal distribution, as well as for the stationarity time. From our analysis we can conclude that the IEEE 802.11p standard will be robust towards inter-symbol and inter-carrier interference inside a tunnel.

I. Introduction

The in-tunnel radio propagation characteristics are peculiar and differ from the typical ones for "open-air" situation. It is of great importance for intelligent transportation systems (ITS) to get a good understanding of them. Applications of reliable *in-tunnel* vehicle-to-vehicle communication are, for instance, lane change assistance, cooperative forward collision warning, or slow vehicle warning, among others. There are only few published studies of in-tunnel vehicular measurements, e.g. [1], [2], [3], [4]. They present results on path-loss and delay spread, but most of them consider only infrastructure-to-vehicle communications and do not use the carrier frequency dedicated for ITS.

Contributions of the paper: In this paper we take the time variation of the channel parameters into account and present an extensive analysis both in the delay and Doppler domain. Furthermore, we evaluate the stationarity time, during which we consider that the statistical properties of the fading process random process remains constant. We evaluate these parameters for a whole measurement set consisting of 7 measurement runs. They all were taken for the *in-tunnel* scenario under several conditions, i.e., different distance between vehicles, constant or increasing speed, with and without cars driving beside. First, we present the detailed results for a representative vehicle-to-vehicle measurement, and afterwards we provide a statistical analysis of the 7 measurement runs.

Organization of the paper: A short description of the in-tunnel scenario is given in Section II. In Section III, we describe the delay and Doppler time-varying parameters, as well as the stationarity time. The results and discussion are presented in Section IV. Section V closes the paper with the concluding remarks.

This research was supported by the projects COCOMINT and NOWIRE funded by Vienna Science and Technology Fund (WWTF), and the EC under the FP7 Network of Excellence projects NEWCOM++. FTW is supported by the Austrian Government and the City of Vienna within the competence center program COMET.

II. In-Tunnel Measurements

The measurements used in this paper were collected in the DRIVEWAY'09 measurement campaign [5]. The tunnel in which the measurement were carried out was the Oresund tunnel, connecting Denmark and Sweden. A total number of 7 measurement runs were performed in order to characterize the radio channel. The channel impulse response $h(t, \tau)$ is measured over $10\,\mathrm{s}$ intervals, each of which contains $S = 32500$ snapshots with a snapshot repetition time of $307.2\,\mu s$. The used carrier frequency is $5.6\,\mathrm{GHz}$ with a bandwidth of $240\,\mathrm{MHz}$. The transmitter (Tx) and the receiver (Rx) cars were equipped with a linear antenna array with 4 elements each. The antennas are circular patch elements with directional radiation patterns, each element is mainly radiating in one of the four main directions: front, back, left, and right, thus covering $360°$ in the azimuth plane. This allows measuring 16 individual impulse responses of the channel, recorded as $h_l(t, \tau)$, where $l = 1 \ldots 16$ represents the link number.

The measurements were performed under various conditions, e.g. different separation distances between Tx and Rx, both cars in the tunnel, one car in the tunnel and the other entering.

We present a detailed analysis of one representative measurement run, where the Tx is already inside the tunnel and the Rx enters it around $2\,\mathrm{s}$ later. The distance between cars is approximately $120\,\mathrm{m}$ and the speed remains constant between

978-1-4244-8331-0/11/$26.00 ©2011 IEEE

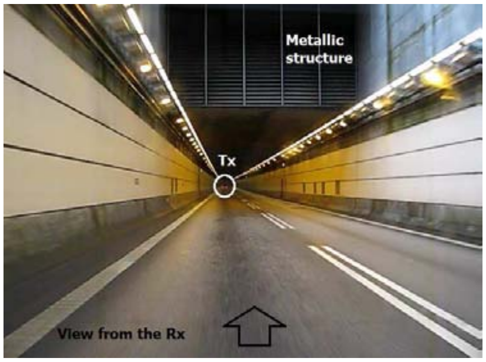

(a) View 1, Rx has not entered the tunnel yet.

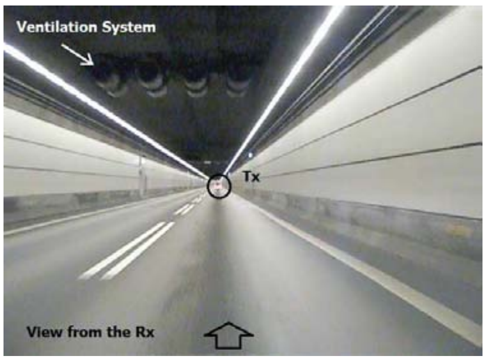

(b) View 2, Tx and Rx are inside the tunnel.

Fig. 1. Pictures taken during the measurement run 1.

100 and 110 km/h. Figure 1 shows two pictures of the view seen from the Rx, driving behind the Tx. The picture in Fig. 1 (a) was taken at the beginning of the measurement, when the Rx is still outside the tunnel. The second picture was taken inside the tunnel, Fig. 1 (b).

III. Time-varying Channel Parameters

For the analysis, we estimate the local scattering function (LSF), introduced in [6] as a useful quantity for characterizing time-varying channels. The LSF is a short-term representation of the power spectrum of the observed fading process in the delay (τ) and Doppler (ν) domain. We calculate the LSF of each individual link and sum them up. By projecting the LSF in the delay or in the Doppler domain, we define the time-varying power delay profile (PDP) and the time-varying Doppler power spectral density (DSD).

Delay and Doppler channel parameters: We use the PDP and the DSD for estimating the root mean square (rms) delay and Doppler spreads (σ_τ and σ_ν), and the excess delay and maximum Doppler dispersion (τ_{exc} and ν_{exc}) respectively. In order to avoid spurious components, we set all the components to 0 which are (i) below the noise power plus 5 dB, and (ii) below the maximum value at a given time instant minus 40 dB, due to the receiver sensitivity. Then we calculate the rms spread values in the same way as it was done in [7].

We are also interested in the excess delay, the difference between the first and the last significant received component; and the maximum Doppler dispersion, the difference between the highest negative and positive Doppler shifts. For that, we define a threshold for which we assume a received signal component to be still relevant, from the receiver point of view. Two thresholds are defined for comparison and are set to 10 and 20 dB respectively below the maximum signal value at a given time instant.

The delay and Doppler parameters are important since they are going to determine whether inter-symbol interference (ISI) and inter-carrier interference (ICI) are going to be present in a given system transmitting through a channel with these characteristics. The conditions for avoiding them are: (i) $\tau_{\text{exc}} <$ guard interval, and (ii) $\sigma_\nu <<$ subcarrier spacing. We compare to the IEEE 802.11p standard meant for vehicular communications, which defines a guard interval of $1.6\,\mu s$, and subcarrier spacing of 156.25 kHz.

Stationarity: The observed fading process in vehicular communications is non-stationary [6]. Therefore, we evaluate the stationarity time, within which one can consider that the fading process remains stationary. The methodology used is based on the collinearity, a bounded similarity measure, which has already been used for assessing stationarity in [8], [9]. The closer to 1 the collinearity is, the more similar the two compared measurements are. On the other hand, a collinearity of 0 means that the two measurements under evaluation are completely different. We consider that two LSFs at two different time instances are similar, when the collinearity between them is equal or greater than 0.9, as done in [9], [10].

For the stationarity analysis we are going to define two stationarity times T_{stat1} and T_{stat2} depending on which measurement data we are using for the calculation, the original one or the line of sight (LOS) delay compensated one. T_{stat1} uses the absolute time scale, i.e., preserving the time-varying delay of the LOS component. However, in a practical Rx, the delay of the first received multipath component (MPC) is estimated and compensated by shifting it to delay 0. We shift the impulse response of each individual link separately. We first detect the delay of the first component higher than the noise power plus 10 dB within a time window of 100 ms, and then shift the whole impulse response by that delay. Considering this setting, we define T_{stat2}, which is going to give more importance on the variations of the later incoming MPC, because the delay of the LOS component is now constant.

IV. Results

In this section, we present the detailed analysis of the time-varying parameters described in Sec. III. In the upper plot of Fig. 2 (a) the PDP is shown, where several contributions are pointed out annotated by roman numerals. The Tx is inside the tunnel and the Rx enters it after approximately 2 seconds. Then, several typical propagation phenomena for in-tunnel scenarios can be observed: (i) multiple signal components parallel to the LOS due to reflections from the tunnel walls and ceiling, (ii) equidistant MPCs caused by reflections on the ventilation system in the tunnel, shown in Fig. 1 (b). In the PDP we can also observe (iii) other MPCs caused by cars

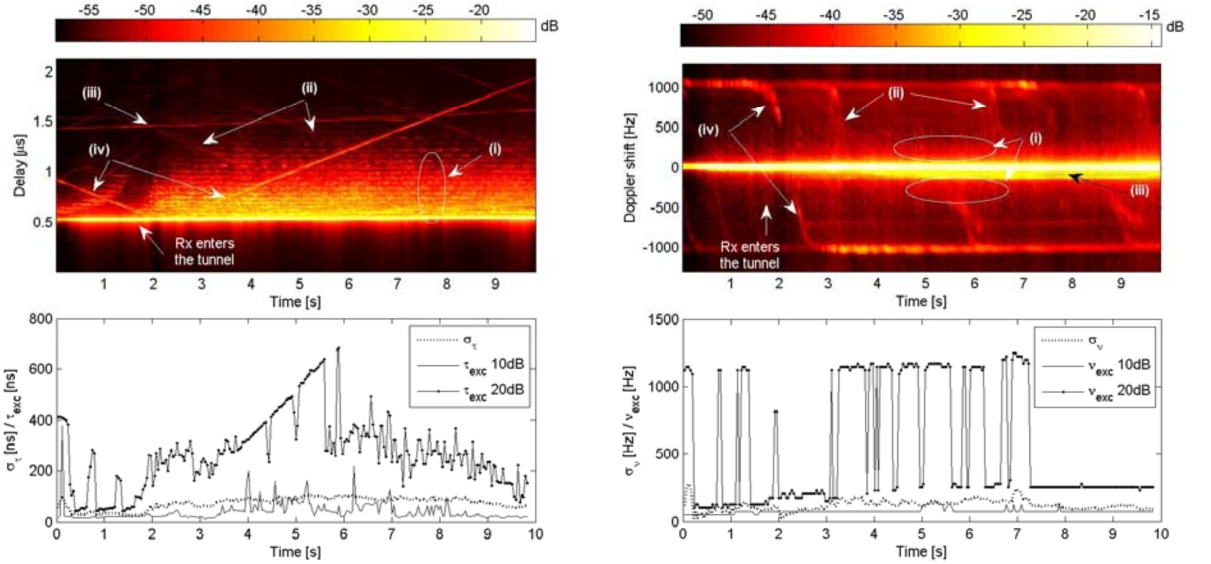

(a) Time-varying power delay profile and delay moments. (b) Time-varying Doppler power spectral density and Doppler moments.

Fig. 2. Time-varying parameters measurement run 1.

driving inside the tunnel, and (iv) a strong MPC caused by a big metallic structure at the entrance of the tunnel, depicted in Fig. 1 (a).

In the lower plot in Fig. 2 (a) the time-varying delay parameters are shown. When both cars are in the tunnel, σ_τ increases and remains more or less constant inside the tunnel, with a maximum value of 107.3 ns and a mean value of 74.5 ns. The $\tau_{\rm exc}$ is evaluated for the two defined thresholds. When considering a threshold of 10 dB, the MPC (ii-iv) are not relevant. On the other hand, when we set the threshold to 20 dB, the MPC (iv) gains importance and strongly influences the $\tau_{\rm exc}$. The strength of MPC (iv) remains higher than the maximum minus 20 dB until approximately 6 s, then, its power falls below this threshold. This is why we observe a big jump at 6 s in the lower plot of Fig. 2 (a), even though we are still able to observe the MPC (iv) in the PDP. The maximum and mean values are summarized in Tab. I. We observe that for this specific measurement, the maximum excess delay is below $1.6\,\mu s$, even considering the worst case with a threshold of 20 dB. In that case, ISI would not be expected.

A similar analysis is performed for the DSD and the Doppler parameters, shown in Fig. 2 (b). Since the Tx and Rx drive in the same direction and more or less at the same speed, the Doppler shift of the LOS component in the DSD remains constant at around 0 Hz. There, the MPCs described in the PDP can also be observed. In Tab. I the mean and maximum values for the Doppler parameters are summarized. The maximum Doppler spread is 280.0 Hz, which fulfills the condition for not having ICI.

Furthermore, we analyze in Fig. 3 the temporal evolution of the stationarity time. We plot the two types of stationarity time defined in Section III. The solid line depicts the absolute time

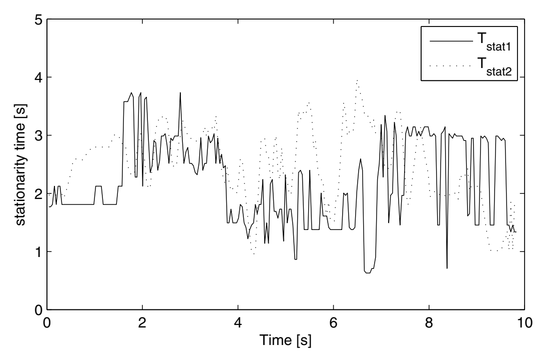

Fig. 3. Temporal evolution of stationarity time for measurement run 1.

TABLE I
TIME-VARYING CHANNEL PARAMETERS FOR MEASUREMENT 1.

Parameters	σ_τ	$\tau_{\rm exc}$ [ns]		σ_ν	$\nu_{\rm exc}$ [Hz]	
	[ns]	10 dB	20 dB	[Hz]	10 dB	20 dB
Mean:	74.51	42.63	273.04	121.13	77.18	549.28
Max:	107.32	379.17	687.50	280.02	152.62	1246.14

version $T_{\rm stat1}$, which oscillates around its mean value at 2.19 s. The shifted time version $T_{\rm stat2}$ is in general larger compared to $T_{\rm stat1}$, because of the constant delay of the LOS component. Its mean value is 2.48 s. Nevertheless, both mean values are relatively close to each other, this is because Tx and Rx drive most of the time at constant speed and constant distance. The stationarity time decreases with increasing strength of the MPC (iv). There are two regions where the influence of this MPC (iv) is weak. Between 2 and 3 s, the metallic structure at the entrance of the tunnel is placed between Tx and Rx. From 7 s, the stationarity time increases again due to the weakness

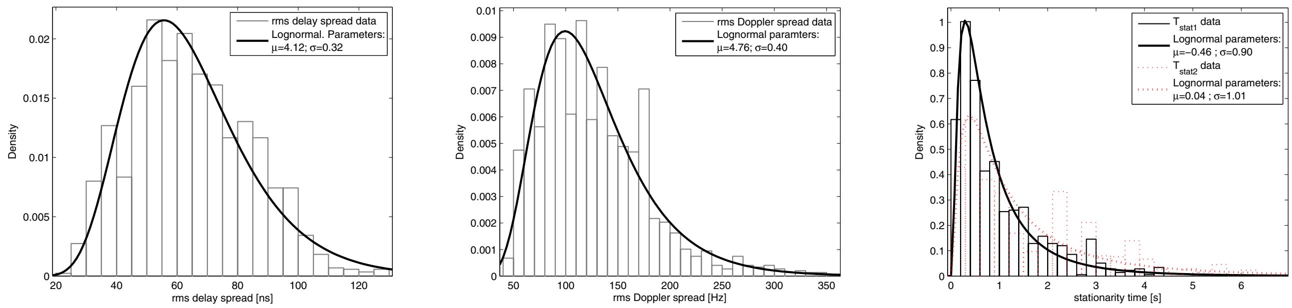

(a) rms delay spreads.

(b) rms Doppler spreads.

(c) stationarity time.

Fig. 4. Stationarity time, rms delay and Doppler spreads histogram and fitted pdf for the whole set of measurements.

of the MPC (iv). We also noticed the influence of MPCs (i), whose presence increases the stationarity time because these MPCs are constant and parallel to each other.

When analyzing stationarity, the most restrictive value is the minimum, in this case found to be $0.63\,\mathrm{s}$ for T_{stat1}, and $0.95\,\mathrm{s}$ for T_{stat2}.

We evaluate the rest of the measurement runs in the same way. The temporal mean values for all of them are summarized in Tab. II. Furthermore, we provide the maximum values for the rms delay and Doppler spreads, and the minimum for the two defined stationarity times. At the end of the table, the mean, maximum, and minimum values for the whole set of measurements are given.

If we want to check whether neither ISI nor ICI would appear in a system transmitting through this channel, we consider the maximum values of the rms delay and Doppler spreads. Considering that the maximum delay excess with a threshold of $10\,\mathrm{dB}$ is about 3 times the rms delay spread, and 6 times with a threshold of $20\,\mathrm{dB}$, we are still under the $1.6\,\mu s$ guard interval specified in the standard. Based on that, we can say that ISI is not going to happen. Regarding ICI, we are considerably far from the maximum tolerable rms Doppler spread, and therefore the system would not suffer under ICI.

We fit the obtained rms spreads to a lognormal distribution [11], and show the good match in Fig. 4 (a) and (b) for rms delay and Doppler spreads respectively. The parameters for the fitted lognormal distribution are ($\mu_\tau = 4.12$, $\sigma_\tau = 0.32$) for the rms delay spread, and ($\mu_\nu = 4.76$, $\sigma_\nu = 0.40$) for the rms Doppler spread. The stationarity time is also lognormal distributed with ($\mu_{T_{s1}} = -0.46$, $\sigma_{T_{s1}} = 0.90$) as parameters for T_{stat1}, and ($\mu_{T_{s2}} = 0.04$, $\sigma_{T_{s2}} = 1.01$) for T_{stat2}.

TABLE II
TIME-VARYING CHANNEL PARAMETERS.

Parameters		σ_τ [ns]	σ_ν [Hz]		T_{stat1}	T_{stat2}
Meas1	Mean:	74.51	121.13	Mean:	2.19	2.48
	Max:	107.32	280.02	min:	0.63	0.95
Meas2	Mean:	68.79	107.05	Mean:	0.59	1.77
	Max:	99.27	358.50	min:	0.08	0.12
Meas3	Mean:	54.87	90.24	Mean:	0.23	0.51
	Max:	95.78	297.77	min:	0.12	0.31
Meas4	Mean:	45.46	132.14	Mean:	0.53	1.03
	Max:	82.13	220.81	min:	0.04	0.47
Meas5	Mean:	75.29	166.44	Mean:	1.92	2.57
	Max:	129.60	331.73	min:	0.31	0.41
Meas6	Mean:	79.20	114.11	Mean:	1.05	2.55
	Max:	109.46	294.39	min:	0.31	0.48
Meas7	Mean:	53.71	46.72	Mean:	0.29	0.50
	Max:	75.38	334.17	min:	0.12	0.20
Total	Mean:	64.55	111.12	Mean:	0.97	1.60
	Max:	129.60	358.50	min:	0.04	0.12

V. CONCLUSIONS

In this paper we presented evaluation results of time-varying channel parameters for vehicle-to-vehicle (V2V) *in-tunnel* radio channel measurements. We identified the most relevant propagation characteristics observed for in-tunnel communications: (i) reflections on walls and the ceiling in the tunnel, (ii) periodic paths coming from reflections on the ventilation system inside the tunnel. Besides them, we also noticed scattering contributions already observed in V2V communications, such as reflections on other vehicles and traffic signs.

The root mean square (rms) delay and Doppler spreads showed a time-varying behaviour with higher values when both vehicles are inside the tunnel. The excess delay and maximum Doppler dispersion are also time-varying and highly dependent on the chosen threshold for their calculation. Furthermore, we evaluated the time evolution of the stationarity time, showing that it is larger when the two cars drive in the same direction with constant speed. We also pointed out the influence of late strong multipath components, and showed that the parallel and constant multipath components, typically observed in *in-tunnel* conditions, increase the stationarity time. When considering a real receiver, the first path detected by the receiver is going to be shifted to delay position 0, therefore, we analyzed as well the stationarity time under this setting and observed that it is larger than considering the absolute time scale.

Since we had 7 measurement runs taken under in-tunnel conditions, we used them for characterizing the distribution of the time-varying parameters analyzed. The rms delay and Doppler spreads, as well as the stationarity time are lognormal distributed.

References

[1] F. Pallares, F. Juan, and L. Juan-Llacer, “Analysis of path loss and delay spread at 900 MHz and 2.1 GHz while entering tunnels,” *Vehicular Technology, IEEE Transactions on*, vol. 50, no. 3, pp. 767 –776, May 2001.

[2] D. Dudley, M. Lienard, S. Mahmoud, and P. Degauque, “Wireless propagation in tunnels,” *Antennas and Propagation Magazine, IEEE*, vol. 49, no. 2, pp. 11 –26, April 2007.

[3] A. da Silva and M. Nakagawa, “Radio wave propagation measurements in tunnel entrance environment for intelligent transportation systems applications,” *Intelligent Transportation Systems, IEEE Proceedings*, pp. 883 –888, August 2001.

[4] G. Ching, M. Ghoraishi, M. Landmann, N. Lertsirisopon, J. Takada, T. Imai, I. Sameda, and H. Sakamoto, “Wideband polarimetric directional propagation channel analysis inside an arched tunnel,” *Antennas and Propagation, IEEE Transactions on*, vol. 57, no. 3, pp. 760 –767, March 2009.

[5] A. Paier, L. Bernadó, J. Karedal, O. Klemp, and A. Kwoczek, “Overview of vehicle-to-vehicle radio channel measurements for collision avoidance applications,” *Vehicular Technology Conference (VTC 2010-Spring), 2010 IEEE 71st*, May 2010.

[6] G. Matz, “On non-WSSUS wireless fading channels,” *IEEE Transactions on Wireless Communications*, vol. 4, pp. 2465–2478, September 2005.

[7] L. Bernadó, T. Zemen, A. Paier, G. Matz, J. Karedal, N. Czink, C. Dumard, F. Tufvesson, M. Hagenauer, A. F. Molisch, and C. F. Mecklenbräuker, “Non-WSSUS vehicular channel characterization at 5.2 GHz - coherence parameters and channel correlation function,” in *Proc. XXIX General Assembly of the International Union of Radio Science (URSI)*, Chicago, Illinois, USA, August 2008.

[8] O. Renaudin, V.-M. Kolmonen, P. Vainikainen, and C. Oestges, “Non-stationary narrowband MIMO inter-vehicle channel characterization in the 5-GHz band,” *Vehicular Technology, IEEE Transactions on*, vol. 59, no. 4, pp. 2007 –2015, May 2010.

[9] A. Paier, T. Zemen, L. Bernadó, G. Matz, J. Karedal, N. Czink, C. Dumard, F. Tufvesson, A. F. Molisch, and C. F. Mecklenbräuker, “Non-WSSUS vehicular channel characterization in highway and urban scenarios at 5.2 GHz using the local scattering function,” in *Workshop on Smart Antennas (WSA)*, Darmstadt, Germany, February 2008.

[10] A. Ispas, G. Ascheid, C. Schneider, and R. Thomä, “Analysis of local quasi-stationarity regions in an urban macrocell scenario,” in *Vehicular Technology Conference (VTC 2010-Spring), 2010 IEEE 71st*, May 2010.

[11] L. M. Correia, “COST 273 Final Report: Mobile Broadband Multimedia Networks,” 2006.